

Characterization of a hybrid nano-silica waterborne polyurethane coating for clay bricks

Original

Characterization of a hybrid nano-silica waterborne polyurethane coating for clay bricks / Pagliolico, SIMONETTA LUCIA; Ozzello, ELENA DANIELA; Sassi, Guido; Bongiovanni, Roberta Maria. - In: JOURNAL OF COATINGS TECHNOLOGY AND RESEARCH. - ISSN 1945-9645. - ELETTRONICO. - 13:1(2016), pp. 1-10. [10.1007/s11998-015-9758-0]

Availability:

This version is available at: 11583/2628430 since: 2016-02-24T13:33:21Z

Publisher:

Springer

Published

DOI:10.1007/s11998-015-9758-0

Terms of use:

This article is made available under terms and conditions as specified in the corresponding bibliographic description in the repository

Publisher copyright

Springer postprint/Author's Accepted Manuscript

This version of the article has been accepted for publication, after peer review (when applicable) and is subject to Springer Nature's AM terms of use, but is not the Version of Record and does not reflect post-acceptance improvements, or any corrections. The Version of Record is available online at: <http://dx.doi.org/10.1007/s11998-015-9758-0>

(Article begins on next page)

CHARACTERIZATION OF A HYBRID NANO-SILICA WATERBORNE POLYURETHANE COATING FOR CLAY BRICKS

Simonetta Lucia Pagliolico^a, Elena Daniela Ozzello^a, Guido Sassi^{a,b}, Roberta Bongiovanni^a

^a Politecnico di Torino, Dept of Applied Science and Technology, C.so Duca degli Abruzzi 24, 10129 Torino, Italy.

^b Istituto Nazionale di Ricerca Metrologica (INRIM), Strada delle Cacce, 91, 10135 Torino, Italy.

Correspondence to: E. D. Ozzello (E-mail: elena.ozzello@polito.it)

ABSTRACT

A transparent hybrid organic-inorganic waterborne coating is evaluated for the protection of clay bricks. The nanocomposite film was prepared by combining an environmental friendly process based on UV-curing of water based acrylic resins and a mild thermal treatment to form nanosilica in situ from alkoxysilane precursors. Coated and uncoated facing bricks were compared by scanning electron microscopy, surface profilometry, water wettability and capillary rise tests. The hybrid coatings acts as a moderate water repellent: interestingly no appreciable alteration of the aesthetical properties of the brick was observed, in particular no gloss and colour change appeared after the treatment.

KEYWORDS

Waterborne photo cured coatings, Polyurethanes protective coatings, Hybrid organic-inorganic coatings, Nanosilica, Clay brick.

INTRODUCTION

Direct exposure to weathering and air pollutants soon causes serious damages to brick masonry¹. The most diffuse degradations of facing bricks are lacunas, pulverization, delamination, cracking, presence of efflorescences, patina and black crusts and dissolution and leaching of mortar between brick courses as one can see in Figure 1.



(a)

(b)

(c)

Figure 1. Facing brick degradations: (a) efflorescence, (b) lacunas and delamination, (c) patinas and black crusts.

It is well known that condensed water is one of the main causes of decay and hindering water penetration is relevant for the protection of porous ceramics. In fact the total open porosity of bricks which controls water penetration severely affects their durability; the presence of pores smaller than 1.5 microns can have a negative influence due to the dynamics of the condensed water circulation within the pore structure and the generation of high crystallization pressures associated to soluble salts and freeze–thaw cycles. In both cases, crystallization pressure is inversely proportional to the pore radius²⁻⁴.

Also the material morphology and the texture of the architectural surfaces deeply influence bricks durability: the formation of black crusts and patina and the cleanability of the altered surfaces depend on these characteristics. Organic and inorganic particulate suspended in the atmosphere can soil surfaces through wet deposition, both causing aesthetic damage (blackening) and creating conditions for oxidation, salt crystallization and black crusts formation (which is a sulphurisation process accompanied by the adhesion of black particles onto the brick). Soil-repelling properties are desired, they depend on the composition of the material exposed to the environmental agents but also on its roughness which includes the finest irregularities of a surface and depends on the chemical and mineralogical composition of the material, on the type and conditions of the production process⁵. Besides being related to the susceptibility of the surface to decay⁶⁻⁸ roughness also affects the optical properties of a material: gloss and colour saturation varies when roughness increases, because of the enhancement of reflected light and the reduction of subsurface light scattering⁹. Furthermore, roughness can cause water detection and the change of the water absorption speed, changing in turn the surface colour¹⁰.

A successful strategy to protect materials from weathering and pollution is the application of a coating¹¹. In the case of natural and artificial building stones, coatings can act both as water-repellent, and as consolidant (adhesive) to preserve the damaged materials and to reduce the decay rate of the material surfaces. Different types of colourless coatings for brick masonry are available, in architecture they are commonly classified as film formers (e.g. acrylics, mineral gum waxes, stearates and urethanes) and penetrants (e.g. methyl siliconates, silanes, alkoxysilanes, silicates) and may be either waterborne or solvent-borne. Manufacturers are now increasingly producing waterborne coatings, which are environmental friendly products: assuring a low emission of volatile organic compounds (VOC) they address the ecological issues and are the preferred choice for obtaining the labelling of green building. Coatings can prevent water penetration, repel contaminants, increase cleanability. At the same time they must not clog pores inhibiting the evaporation of water and causing clouding and spalling of the brick: coatings must coat but not occlude the pores allowing a good breathability of the masonry wall.

The choice of a coating should also respect compatibility criteria, especially in the field of conservation and restoration. Compatibility between the coating and the original material is a key issue and treatments should only slightly alter the characteristics of the original material, leaving the material similar to the uncoated substrate. Unfortunately the formation of a polymeric film effective at preventing water and contaminants from penetrating into brick, and at increasing its cleanability, many times produce changes in colour and gloss.

In other words coatings for porous materials should provide impermeability to liquid water, permeability to water vapour, oil repellence, no colour change, chemical inertness, environmental stability and energy saving^{12,13}. On the bricks protection by coating several interesting studies have been published over the past decades. In 1970 Ashton¹⁴ investigated the applicability of paints on brick surface not only for aesthetical purposes, but also for protection. Franke and Pinsler¹⁵ stated that water repellents should not be used on masonry containing soluble salts where the risk of capillary rise exists, especially in the case of decorated brick, and spalling phenomena can take place as a function of the depth of penetration of the water repellent product. Van Hees et al.¹⁶ observed that the severity of the damage caused by salts is

dependent on the depth of penetration of the treatment: the deeper the penetration, the more severe the damage at a longer time. Later, Defreese and Charola¹⁷ showed that silicate-based mineral paints and acrylic latex paints were water-vapour-permeable and could reduce water infiltration from driving rain, displace the crystallization front up to the brick surface, reduce the depth of the damaged zone, increase the life of the brick, also providing a visible warning of deterioration by the spalling of the coating. Moreover when the paints peeled off the substrate, there was no damage to the brick and the treatment could be reversible. Enhancement of the hydrophobic properties without affecting breathability was also observed treating samples by alkoxysilanes: a significant decrease of the masonry water content was obtained and at the same time an improved thermal insulation of the brickwork¹⁸. Improvement in both water absorption and mechanical properties were achieved treating tiles with acrylic polymers, among which the best known is poly-ethyl methacrylate-co-methyl acrylate (Paraloid B-72)¹⁹. Interesting publications evaluate the capillary water absorption of untreated and coated clay bricks^{12, 16, 20-24}, however only few literature data can be compared because different standards were followed for capillary water absorption measurement and there is great variability in the water absorption curves.

Because of its transparency and versatility conservators have been widely using acrylics to protect ceramics. More recently polyurethane-based film formers (PU) are finding acceptance as water repellents for building materials: they can provide a good gloss and better durability, adhesion and mechanical properties if compared with other resins²⁵⁻²⁷ finding application as anti-corrosion coatings²⁸ and coatings for wood²⁹.

Polyurethanes water based dispersions are also available: they are ionomeric structures in which the polymeric backbones bear carboxylic or quaternary ammonium groups acting like internal emulsifiers and allowing to disperse the hydrophobic polymer in water. Monocomponent waterborne polyurethanes are largely thermoplastics: due to their macromolecular nature it can be difficult to assure penetration and linkage onto the porous ceramic structures of masonry materials; the use of lower molecular weight structures with lower viscosity cured in situ is preferred. PU oligomeric structures can be functionalized to be crosslinked and PU end-capped by (meth)acrylic functions are curable by light in the presence of radical photoinitiators³⁰⁻³¹. The process usually relies on UV irradiation and is known as UV-curing. However more recently initiating systems sensitive to visible light have been tested and curing under solar irradiation is possible³²⁻³⁴. The photo-curing (both under UV and visible light) allows bulk polymerization in a very short time (seconds of radiation instead of hours of thermal treatment), so that a wide variety of applications are on the market.

Improvements of the mechanical performances of the PU coatings have been achieved by dispersing inorganic nanoparticles in the organic matrix³⁵ or by adding inorganic precursors, to generate nanoparticles via sol-gel processes performed in situ. In particular, UV-cured waterborne polyurethane acrylic coatings containing nanosilica have been prepared in a previous work by means of a dual-curing process and coatings have been applied to metal substrate to protect from corrosion³⁶.

No literature data have been found referring to the application of water borne photocurable PU acrylic resins on brick substrate having a porous texture, while interesting results were reported on UV-cured nanocomposite coatings based on trimethylolpropane trimethacrylate and a vinyl terminated polydimethylsiloxane applied to porous stones³⁷.

In this work nanostructured hybrid silica/polyurethanes has been used to treat modern facing clay bricks, in order to analyse its applicability on brick surface as protective coating. Coated and uncoated brick samples were characterized by means of XRD, scanning electron microscopy (SEM), and mercury intrusion porosimetry (MIP). Surface profilometry, water absorption, gloss and colour measurements were also

performed in order to investigate the water repellency of the resin and to evaluate the compatibility between the coating and substrate.

EXPERIMENTAL

Specimen preparation

A commonly used commercial red facing clay brick has been selected as substrate. Prismatic samples at nominal size 10x20x30 mm were cut by a miter saw REMET TR 100S, meeting the UNI EN 772-16:2002 standard³⁸. Each specimen was washed in running water, cleaned by a soft brush, and soaked in deionized water for 30 min. Samples were then dried at 60 (± 2) °C till constant weight (i.e. until the difference between two weighing at an interval of 24 h was not greater than 0.1 % of the mass of the specimens), and stored in a desiccator with silica gel at room temperature. The mineralogical composition of the clay brick (XRD analysis), the total intruded porosity (TIP) and mean pore size (MPS), the capillary water absorption coefficient (AC), the gloss (G), the surface roughness (Ra), the water contact angle (θ) and the colour were measured on the substrate. Four samples were treated with a UV-curable organic-inorganic hybrid nanosilica waterborne polyurethane resin (OIH).

The OIH resin was prepared adding drop by drop a water solution of NH_4OH to the water based ionomeric polyurethane diacrylate (trade name UCECOAT 6558, MW @ 10,000 g/mol, kindly given by Allnex, USA) till a final pH value of 9. 20 wt % of tetraethoxysilane (TEOS) and 3 wt % of Darocur 1173 photo-initiator were added to the mixture under vigorous stirring. The resins were applied onto the surface of the brick specimens in several runs (from 3 to 4 times, wet on wet, until rejection), by bar-coating (200 μm coating bar); the bricks were dried in oven at the temperature of 60°C for 30 min to induce the evaporation of water. The treated face of each sample (20 x 30 mm) was finally exposed to UV irradiation in a N_2 atmosphere by means of a medium pressure mercury lamp at the intensity of 25 mW cm^{-2} at the sample level for 2 min.

The same procedure was adopted to prepare an OIH coating on a glass slide.

Treated samples were dried at 60 (± 2) °C until constant weight and stored in a desiccator with silica gel at room temperature.

The amounts of OIH absorbed by brick samples until rejection per unit surface were calculated as the difference of the specimen mass (kg) before and after impregnation and curing, divided by the treated surface area (m^2). No resin and no wax or any other sealant was used to coat the other surfaces of the samples.

Analyses and characterization

XRD patterns were recorded with a Philips PW 1710 diffractometer between 5° and 70° in 2θ , with a step width of 0.04° and 2.5 s data collection per step ($\text{CuK}\alpha$ radiation and graphite secondary monochromator). Three untreated samples were first roughly crushed together in an agate mortar with an agate pestle and the powders were sieved with steel meshes having apertures of 0.105 mm. The passing fraction at 0.105 mm was used to determine the mineralogical composition of the brick. The total intruded porosity and the pore size distribution were measured with an Hg Porosimeter (Carlo Erba PO2000 with macropore unit) on three brick fragments (weighing less than 1 g) obtained from three different samples. The maximum pressure reached during the analysis was 800 bar.

The OIH coating prepared on a glass slide was analysed by transmission electron microscopy TEM after an Ar ion polishing (GATAN PIPS system, working at 3.5 keV at an angle of 7°). They were examined in a 300-

keV TEM Philips CM30. TEM micrographs were processed with a slow scan CCD camera and analysed with the Digital Micrograph program. The TEM observations were always performed using a very low electron flux in order to avoid any structural modification of the sample induced by the electron beam.

SEM analyses were carried out on metallized untreated samples (Cr, 9-11 nm) in order to evaluate the morphology of brick surface (FEI Quanta inspect 200 LV operated at 15 kV, 100 μ A, in an ultra-high vacuum, 1.5×10^{-5} mbar). Two cross sectioned slices (3 mm thick) were cut by a miter saw REMET TR 100S from the fourth brick sample treated by OIH. One slice was subjected to extraction with chloroform to eliminate the uncured resin. The sample was wrapped in a fine metallic mesh, immersed in chloroform for 24 h at room temperature, then dried in an oven at 80 °C for 6 h and observed by SEM after metallization. The depth of penetration of the resin inside brick slices was visible on SEM micrographs; it was measured by mean of a digital pointer with 1 μ m reproducibility and 10 μ m was assumed as uncertainty of the depth of penetration measurement. A set of 30 measurements has been made on the cross section edge of the two specimens (20 mm length). Variability of the depth of penetration along the section was calculated as uniformly distributed between the maximum and minimum values³⁹⁻⁴⁰. Total uncertainty of the depth measurement was calculated combining reproducibility of pointer, uncertainty of placement and variability of the measured depth along the section³⁹⁻⁴⁰.

The water absorption coefficient of both treated and untreated samples was measured by using a gravimetric sorption technique according to UNI EN 15801:2010⁴¹. Three untreated specimens and three specimens treated by OIH were tested. The same samples were tested for gloss, contact angle, and colour change measurements. The initial weight of the prismatic specimens was measured and each sample was positioned inside a closed container with the treated surface facing a stack of filter papers (Whatman 4) soaked with deionized water. At different times each specimen was weighted after removing water from the surface by a damp cloth. The measurements were stopped when the weight change over 24 h was less than 1 wt % of the mass of water absorbed by the specimen⁴¹.

Water content per unit surface area Q_i at time t_i was calculated as $Q_i = (m_i - m_0)/A$, where m_i is the mass of the specimen at time t_i (kg); m_0 is the constant mass of the dry specimen; t_i is the time elapsed from the beginning of the test (s); A is the area of the specimen in contact with water (m^2)⁴¹.

The absorption coefficient (AC) values were calculated as the slope of the linear section of the $Q = f(t^{1/2})$ curve by a linear regression of the least 5 successive aligned points ($R^2 \geq 0.99$; slope uncertainty was calculated to be lower than 0.01 kg m^{-2})³⁹⁻⁴¹.

Total uncertainties of Q_i were calculated combining measurement uncertainty and sample variability^{39,40}. Measurement uncertainty was calculated combining standard uncertainty of the direct measurement of mass, dimension and time^{39,40}. Time standard uncertainty was less than 10 s, dimension standard uncertainty was less than 0.3 mm, dry sample mass uncertainty was less than 0.001 g. Wet sample mass standard uncertainty was estimated to be 0.06 g. Wet sample mass uncertainty resulted to be the most relevant contribution to measurement uncertainty.

The protection degree by capillarity (PD_C) was estimated, by comparing the amount of water absorbed before (Q_{bt}) and after the treatment (Q_{at}): $PD_C = (Q_{bt} - Q_{at})/Q_{bt}$ ⁴². Measurement uncertainty and variability of PD_C were considered separately^{39,40}.

Contact angle measurements were performed at room temperature using the sessile drop technique by mean of the drop shape analyser DSA100 Kruss-GmbH instrument (UNI EN15802:2010 standard⁴³). The measuring liquid was bi-distilled water (surface tension $\gamma = 72.1 \text{ mN m}^{-1}$). The results were the mean values of 3 measurements on each of the three treated sample (nine measurements).

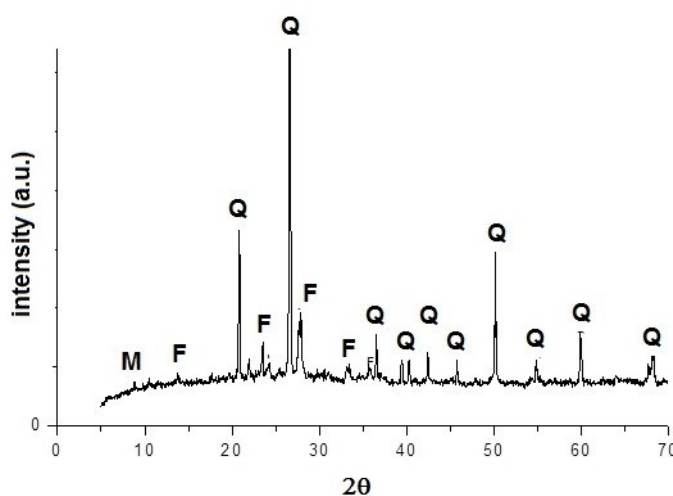
The surface roughness was measured by profilometry (three measurement for each series of samples). A SurfTest 201 Series 178 Mitutoyo instrument with a stylus tip radius of 2 μm was used for the measurements adapting the method for advanced monolithic ceramics described in UNI EN 623-4:2005 standard⁴⁴. Samples were scanned (with a traverse speed of 0.5 mm s⁻¹) over a sampling length of 7.5 mm along six X-lines and Y-lines for each sample using a grid with a step size of 1.5 mm (0, 1.5 mm, 3 mm, 4.5 mm, 6 mm and 7.5 mm). R_a (in μm) was chosen to compare samples roughness before and after treatment: R_a was calculated as the arithmetic mean of the absolute values of the deviations from the average centerline and described the average height or depth of the peaks above and below the centerline. A mechanical filter with long wavelength cut-off equal to 2500 μm was used to separate macro roughness (waviness) from micro roughness. Cut-off length was established according to the instrument setting limitations and assessing the roughness of brick samples by SEM micrographs. The R_a values presented in this paper were calculated as the average values from both the X and Y line profiles for each specimen and the spatial grid was used to ensure repeated measurements after treatment on the same points in subsequent tests.

The effect of the coatings on the optical properties of the samples was evaluated by measuring their gloss. A P. Zehntner testing instruments ZGM 1020 Glossmeter 60° was used to measure the gloss of treated and untreated samples according to ISO 2813:1994⁴⁵. Measurements were repeated 3 times for each specimen being the specimen surface entirely covered by the measurement area of instrument. The average results (three measurements) were expressed in gloss units (GU). Colour measurement of untreated and treated brick surfaces was carried out by means of a portable spectrophotometer MINOLTA CM-508d in diffuse reflectance. The instrument measures the spectral reflectance of the samples in double channel mode under a white light generated by an in-built xenon lamp. The determinations were carried out according to UNI EN 15886:2010⁴⁶. The spectral reflectance was measured at a 20 nm pitch from 400 to 700 nm and the colour changes were evaluated through the L*a*b* system (ASTM D-1925, CIE 1976) and expressed as ΔE .

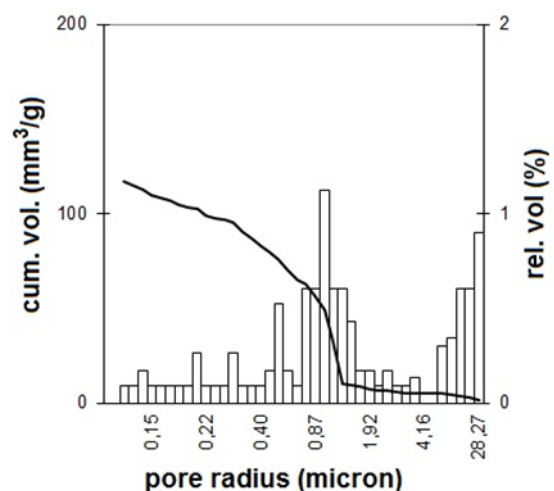
RESULTS AND DISCUSSION

Characterization of the brick substrate

XRD analysis on the uncoated brick (Figure 2a) revealed the presence of intense quartz lines (Q), and the presence of calcium feldspar (anorthite, albite) (F) and mica (M), which are typical constituents of traditional clay bricks.



(a)

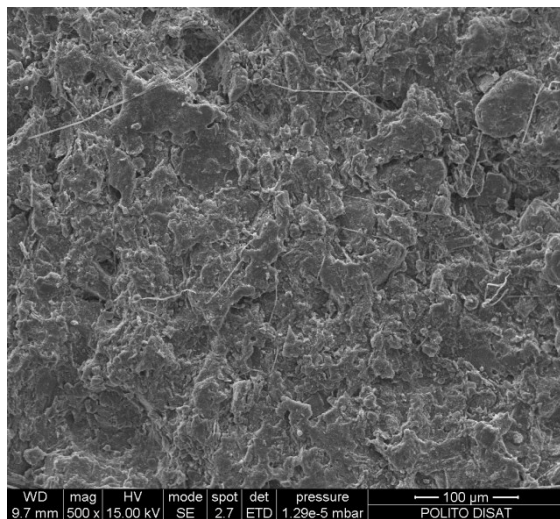


(b)

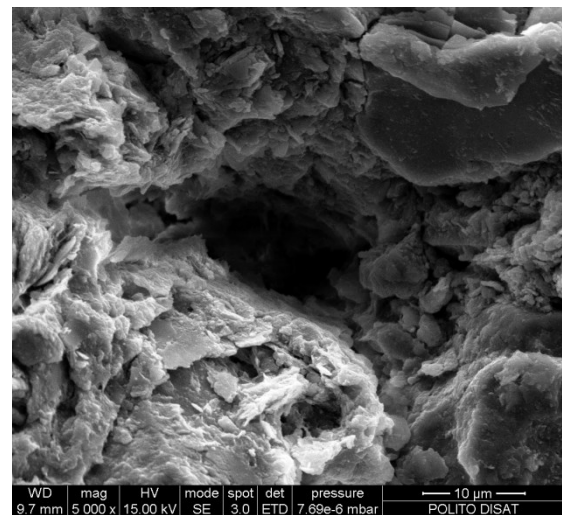
Figure 2. Characterization of clay bricks: (a) Powder diffraction pattern of untreated brick. F=feldspar, M=mica, Q=quartz. (b) MIP pore radius distribution of an untreated brick sample.

MIP pore radius distribution of uncoated brick samples (Figure 2b) showed a clear bimodal distribution with a mean pore radius of $1.07\ \mu\text{m}$ and an average total accessible porosity equal to 31.7 %, as commonly found for solid brick porosities². There is the presence of pores smaller than $1.5\ \mu\text{m}$: as discussed in the introduction this may negatively affect bricks durability as crystallised water produces a pressure inversely proportional to the pore size.

SEM micrographs reported in Figure 3 show the surface of an untreated brick sample (Figure 3a) and the morphological aspect of the open pores (Figure 3b). In Figure 4 a representative X-line profile of the surface roughness of an untreated sample (Figure 4a) is reported together with the SEM micrograph (Figure 4b). The Ra value resulted lower than $10\ \mu\text{m}$ (Table 4 in section 3.3).

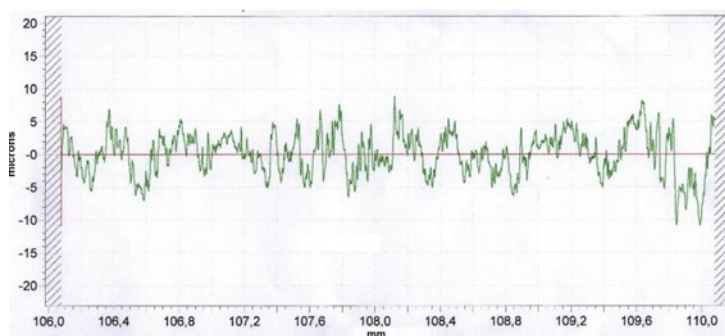


(a)

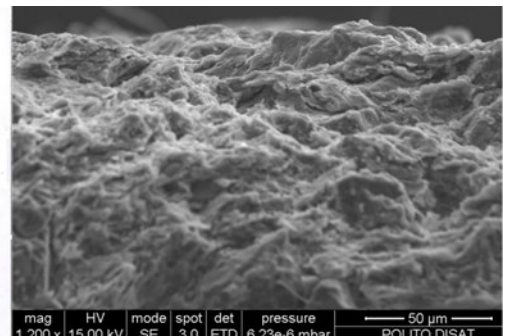


(b)

Figure 3. SEM micrograph of untreated brick: (a) surface roughness (front view, 500x); (b) open pore morphology (5000x).



(a)



(b)

Figure 4. Roughness of clay bricks: (a) Representative X-line profile of untreated sample; (b) SEM micrograph of the surface roughness (lateral view, 1200x).

Characterization of OIH resin

As described in a previous work³⁶, the OIH coating can be prepared combining a sol-gel process to form silica from liquid alkoxysilane precursors and a photoinduced reaction to crosslink the acrylic binder embedding the inorganic nanoparticles.

The morphology of the hybrid coatings prepared in the present work was investigated by TEM microscopy. Figure 5 shows the TEM micrograph of silica nanoparticles contained in a thin film of resin coated and cured onto a glass slab through the dual-curing process. The photo reveals the size of the individual silica nanoparticles having an average diameter of 40-50 nm. Thus an organic-inorganic nanostructures network is obtained; nanosilica is formed and is expected to enhance the chemical affinity of the coating towards the brick substrate which contains quartz. The presence of silica also enhances several properties of the coatings: OIH shows better mechanical properties and better thermal stability than the silica-free homologue (anyway for both coatings the onset of thermal degradation in air is above 100°C, in agreement with previous results³⁶); as the particles size is nanometric, OIH maintains a good optical transparency. The glass transition temperature of OIH is 73 °C measured by dynamic mechanical analysis, the crosslinking density calculated from the storage modulus at the rubbery plateau is 4.45 mmol cm⁻³³⁶.

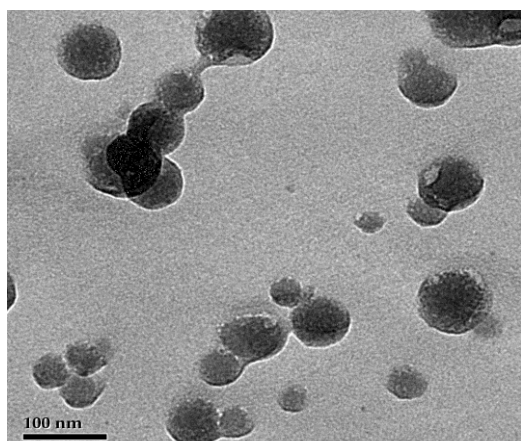


Figure 5. TEM image of OIH resin: sample prepared from polyurethane diacrylate + 30% TEOS coated onto a glass substrate.

Characterization of treated brick samples compared to the untreated

The brick samples were treated with the OIH formulation until rejection following the procedure reported in detail in the experimental part: first the liquid reactive mixture was coated onto the brick, then the sample was heated to remove water, finally it was irradiated for inducing the curing of the acrylic oligomer and then heated again to complete the sol-gel process forming the silica. The average amount of OIH resin present in the brick after the whole treatment was 0.063 kg m⁻² which is much lower than the quantity applied by other researchers in similar works³⁷. From SEM analyses carried out on the treated brick sample (Figure 6) no compact film was evident on the surface of the specimen (Figure 6a). However, as clearly evident in Figure 6b, the resin penetrated the brick till an average depth of 730 ± 44 µm. The resin was fully cured, in fact when the specimen was subjected to chloroform extraction, the soluble fraction was negligible and no appreciable difference in penetration depth was observed (average depth value = 682 ± 52 µm). Therefore the resin absorbed by the brick substrate polymerized by irradiation, was well cured (in agreement with results showing that the insoluble fraction of the OIH coating alone is 97%³⁶) and could not be extracted by a solvent. **The same results were obtained using the acrylic resin without the addition of**

TEOS, thus the acrylic network alone , without the inorganic part, can be crosslinked till the bottom of the impregnated layer. Moreover, as after extraction the penetration depth did not change, one can suggest that the coating showed a good adhesion to the brick.

At the same time, as shown in Figure 6c-d, the OIH coating did not occlude the porosity. As discussed in the introduction, these are important requirements in order to respect the criteria of material breathability, compatibility and to prevent the substrate damage.

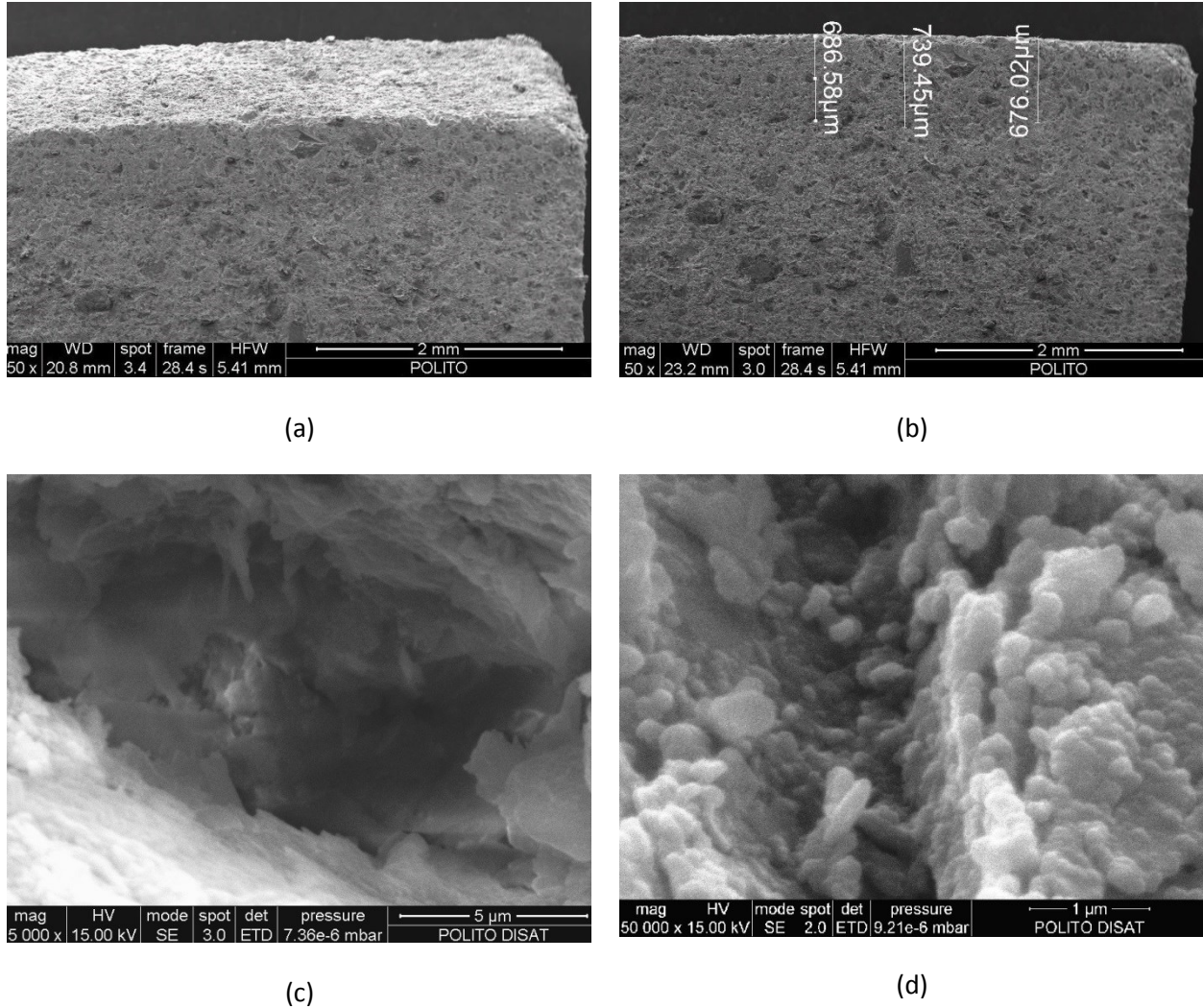


Figure 6. SEM micrographs of brick samples: (a) and (b) treated with OIH until rejection (50x); (c) open porosity of a sample treated with OIH until rejection (15000x); (d) magnification of the pore wall (50000x).

Wettability of the treated brick samples was assessed by considering both the contact angle measurements θ and the capillary water absorption coefficient AC (Table 1). As expected the water contact angle of bricks is not measurable as water penetrated immediately. The contact angle of the treated sample shows a remarkable increase: the value exceeds 90° meaning that the surface is highly hydrophobic. Hydrophobicity is achieved even if the amount of the protective product is very low and its composition does not include strongly hydrophobic agent such as silicone or fluorinated monomers employed by other authors. Since spalling phenomena could take place using strong water repellents¹⁵, depending on the depth of penetration of the coating¹⁶, in the case of brick substrate a coating with a moderate water repellency was considered preferable and the amount of absorbed resin was kept low, carrying out the treatment only

until rejection. Adding hydrophobic functional groups, increasing the content of nanosilica in the formulation of OIH resin, and optimizing nano-particle size distribution, varying the depth of penetration the protective action of coating could be enhanced. In this case, more attention should be paid to degradation phenomena as mentioned in the introduction.

Table 1. Capillary water absorption coefficient and contact angle of treated and untreated brick samples.

Samples	AC ($\text{kg m}^{-2}\text{s}^{-1/2}$)	θ
Untreated	0.094 ± 0.010	(*)
Treated by OIH	0.088 ± 0.010	$108^\circ \pm 2^\circ$

(*) Not measurable

The absorption coefficient (AC) values were calculated as the slope of the linear section of the $Q = f(t^{1/2})$ curves describing capillary absorption as shown in Figure 7. The absorption curves $Q = f(t^{1/2})$ show a sigmoidal trend and three zones can be observed: in the first 2-3 min absorption rates are low and depend on the presence of the coating; after 3 min higher absorption rates are attained and are similar for untreated and treated samples; after 20-30 min the absorption rates slow down. Still the untreated samples show a higher absorption than OIH (see insert). However it is interesting to observe that a time delay for the water absorption appears when the samples are coated. Although uncertainty is relevant, data suggest that the coatings decreases the water absorption: in fact AC value is lower for the coated sample. Analysing literature data, lower absorption was obtained using silanes/siloxanes, yielding to silicone resins¹², and acrylates modified by copolymerisation with hydrophobic monomers³⁷. However, as previously said, only few studies showed results comparable to those obtained in the present work. Referring to untreated brick, Mukhopadhyaya et al.²¹ obtained similar AC value for red clay bricks: from 0.077 to $0.094 \pm 0.009 \text{ kg m}^{-2}\text{s}^{-1/2}$ at 21 °C. Esposito Corcione et al.³⁷ treated with a hybrid methacrylic-based coating a porous stone substrate (*Pietra Leccese*) having porosity similar to the brick samples treated in the present work and a higher AC value. The best water repellency was obtained by Esposito Corcione et al.³⁷ when the average amount of resin used to treat the stone substrate was increased up to 0.4 kg m^{-2} . In the present study a lower amount of OIH resin was absorbed by brick (0.063 kg m^{-2}).

In Figure 8 the average protection degree by capillarity (PD_c) estimated by comparing the amount of water absorbed before and after the treatment, is plotted vs. time. PD_c is around 50 % and then decreases to 4% after 30 min. However the variability of the samples was very high, data clearly indicate that the coating is not highly effective in protection and the optimization of the composition and of the coating process is necessary.

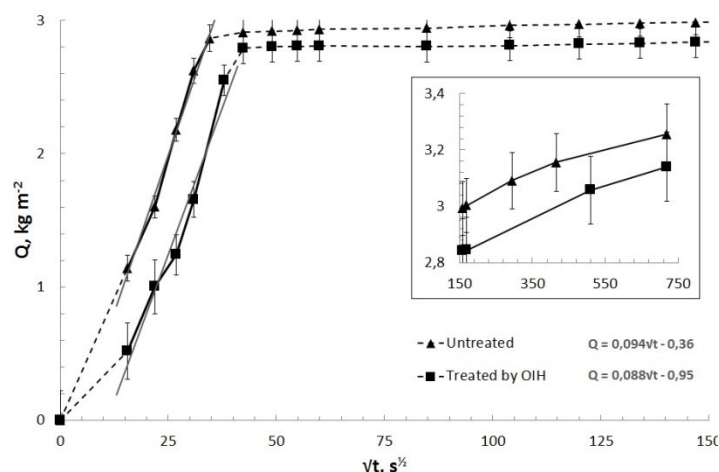


Figure 7. Capillary water absorption of untreated and treated brick samples. (results at longer times in the inset)

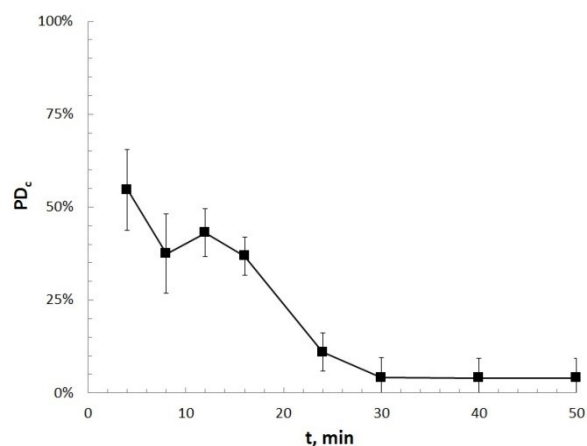


Figure 8. Protection degree by capillarity: first 50 min of the water absorption test.

The surface roughness R_a , the gloss G and the colour of the samples (L^* , a^* and b^* chromatic coordinates and ΔE - CIELAB system), before and after the coating were measured. Data are reported in Table 2 and show that the treatment does not alterate the aspect of the brick, as requested in most applications.

Table 2. Roughness, gloss and colour of the treated and untreated samples.

Sample	R_a (μm)	G (GU)	L^* white	a^* red	b^* blue	ΔE
Untreated	9.0 ± 1.3	<1	40.51	17.55	20.29	0
Treated by OIH	8.9 ± 1.7	<1	39.45	18.74	20.98	1.53

Roughness uncertainty was calculated combining reproducibility and variability; roughness changes between treated and untreated samples are inside the uncertainty.

It is evident that the treatment does not affect roughness. In agreement with this result, gloss is found unchanged after application of OIH coatings. Other interesting results concern colour measurements: no relevant change is measured. In the presence of the coating there is a small variation of L^* and a^* (meaning that the samples become slightly greyer and more red). However the ΔE value is not greater than 2.00: this means that the color difference cannot be perceived by the human eye and that treatment is fully acceptable for restoration and cultural heritage application⁴².

CONCLUSION

Hybrid UV-cured waterborne polyurethane are considered environmental friendly and have proved to be good protective coatings and water repellents for building materials such as metals and wood. Their performances and applicability on brick surface have been tested in this work. These innovative coatings contain nanoparticles synthesized in situ via a sol-gel process, which is combined with the UV-curing step. The hybrid coating, does not change the roughness, the gloss and the colour of bricks, i.e. the aesthetical properties do not vary appreciably after treatment. It was shown that the coatings can be applied on bricks surface till a depth of hundred microns without occluding pores and without forming a compact continuous external layer. Surface wettability of brick samples was substantially decreased and a delay in water

absorption was observed. A tendency to a decrease of the capillary absorption coefficient was also observed. The overall results indicate the possibility of employing these systems to protect clay bricks; optimizing the preparation conditions, the silica content and the nanoparticle size distribution and increasing the process control the performance of the hybrid coating could be further enhanced. The process can be proposed as an additional step in brick manufacturing, alternatively the on-site application of the coating on building brickworks could be foreseen by exploiting the solar radiation for initiating the curing if photo-initiating systems sensitive to longer wavelengths (towards the visible range) will be used. Moreover further characterization will be done, in particular vapour rate transmission tests and mechanical tests are in progress. More attention should also be paid to degradation phenomena.

REFERENCES

1. M. Collepardi, *Mater. Struct.* **1990**, *23*, 81-102.
2. Cultrone, G., Eduardo, S., Elert, K., De la Torre, M. J., Cazalla, O., Rodríguez-Navarro, C. *J. Eur. Ceram. Soc.* **2004**, *24*, 547–564.
3. Rodríguez-Navarro, C., Doehne, E. *Earth Surf. Process Landforms* **1999**, *24*, 191-209.
4. Winslow, D. N., Kilgour, C. L., Crooks, R. W. *Am. Ceram. Soc. Test Mater.* **1988**, 527–531.
5. Vazquez-Calvo, C., Alvarez de Buergo, M., Fort, R., Varas-Muriel, M., J. *J. Geophys Eng.* **2012**, *9*, 108–117.
6. Avdelidis, N. P., Delegou, E. T., Almond, D. P., Moropoulou, A. *NDT & E Int.* **2004**, *37*, 571–575.
7. Kuisma, R., Fröberg, L., Kymäläinen, H.-R., Pesonen-Leinonen, E., Piispanen, M., Melamies, P., Hautala, M., Sjöberg, A.-M., Hupab, L. *J. Eur. Ceram. Soc.* **2007**, *27*, 101–108.
8. Delegou, E. T., Avdelidis, N. P., Karaviti, E., Moropoulou, A. *X-Ray Spectrom.* **2008**, *37*, 435–443.
9. Donner, C. S. Towards Realistic Image Synthesis of Scattering Materials, PhD Thesis. San Diego: University of California; **2006**.
10. Graziani, L., Quagliarini, E., Bondioli, F., D’Orazio, M. *Build. Environ.* **2014**, *71*, 193-203.
11. J. A. Graystone, *Coatings and buildings in: Paint and surface coatings: theory and practice*, R. Lambourne, EDS 383-397, Woodhead Pub. **1990**, Cambridge, UK.
12. Matziaris, K., Stefanidou, M., Karagiannis, G. *Prog. Org. Coat.* **2011**, *72*, 181-192.
13. Sadat-Shojai, M., Ershad-Langroudi, A. *J. Appl. Polym. Sci.* **2009**, *112*(4), 2535-2551.
14. Ashton, H. E. *Can. Build. Dig.* **1970**, *131*, 3-7.
15. Franke, L. and Pinsler, F. *Int. J. Restor. Build. Monum.* **2001**, *4*(5), 187-207.
16. van Hees, R. P. J., Brocken, H. J. P. *Constr. Build. Mater.* **2004**, *18*, 331–338.
17. Defreese, E. S. N. and Charola, A. E. *J. Am. Inst. Conserv.* **2007**, *46*(1), 39-52.
18. MacMullena, J., Zhanga, Z., Rirsch, E., Dhakala, H.N., Bennetta, N. *Energ. Build.* **2011**, *43*, 1560-1565.
19. Constancio, C., Franco, L., Russo, A., Anjinho, C., Pires, J., Vaz, M. F., Carvalho, A. P. *J. Appl. Polym. Sci.* **2010**, *116*, 2833–2839.
20. Delucchi, M., Barbucci, A., Cerisola, G. *Prog. Org. Coat.* **1998**, *33*, 76–82.
21. Mukhopadhyaya, P., Kumaran, K., Normandin, N., Goudreau, P. *J. Therm. Envel. Build. Sci.* **2002**, *26* (2), 179-195.
22. De Clercq, H. Performance of Single Materials Treated with a Water Repellent and Contaminated with a Salt Mix. In: Silfwerbrand J, editor. Proceedings of Hydrophobe IV- the 4th International Conference on Water Repellent Treatment of Building Materials. Freiburg: Aedificatio Publishers; **2005**, p. 171–184.
23. Cultrone, G., Sebastia, E., Ortega Huertas, M. *Constr. Build. Mater.* **2007**, *21*, 40–51.
24. Groot, C. J. W. P., Gunneweg, J. T. M. *HERON* **2010**, *44*(2), 63-78.
25. Chattopadhyay, D. K., Raju, K. V. S. N. *Prog. Polym. Sci.* **2007**, *32*(3), 352-418.

26. Masson, F., Decker, C., Jaworek, T., Schwalm, R., *Prog. Org. Coat.* **2000**, 39(2–4), 115–126.
27. Lee, M. H., Choi, H. Y., Jeong, K. Y., Lee, J. W., Hwang, T. W., Kim, B. K. *Polym. Degrad. Stabil.* **2007**, 92(9), 1677–1681.
28. Xu, J., Rong, X., Chi, T., Wang, M., Wang, Y., Yang, D., Qiu, F. *J. Appl. Polym. Sci.* **2013**, 130(5), 3142–3152.
29. Nguengang, N. W., Riedl, B., Landry, V. J. *Coat. Tech. Res.* **2014**, 11(3), 283–301.
30. Masson, F., Decker, C., Jaworek, T., Schwalm, R. *Prog. Org. Coat.* **2000**, 39, 115–126.
31. Tielemans, M., Roose, P., De Groote, P., Vanovervelt, J. *Prog. Org. Coat.* **2006**, 55, 128–136.
32. Shao, J., Huang, Y., Fan, Q. *Polym. Chem.* **2014**, 5, 4195–4210.
33. Fouassier, J. P., Allonas, X., Burget, D., *Prog. Org. Coat.* **2003**, 47, 16–36.
34. Mauguier-Guyonnet, F., Burget, D., Fouassier, J. P. *Prog. Org. Coat.* **2006**, 57(1), 23–32.
35. Novak, B. M. *Adv. Mater.* **1993**, 5, 422–433.
36. Di Gianni, A., Bongiovanni, R., Turri, S., Deflorian, F., Malucelli, G., Rizza, G. *J. Coat. Tech. Res.* **2009**, 6(2), 177–185.
37. Esposito Corcione, C., Striani, R., Frigione, M. *Prog. Org. Coat.* **2014**, 77, 803–812.
38. UNI EN 772-16:2002. Methods of test for masonry units. Determination of dimensions. **2002**.
39. ISO JCGM 100:2008 Evaluation of measurement data – guide to the expression of uncertainty in measurement. Joint Committee for Guides in Metrology. **2008**.
40. Taylor, J. R. *An Introduction to Error Analysis: The Study of Uncertainties in Physical Measurements*. 2nd ed. Mill Valley: University Science Books; **1997**.
41. UNI EN 15801:2010. Conservation of cultural property - Test methods - Determination of water absorption by capillarity. **2010**.
42. CEN TC346001/WG3 N.120. Conservation of cultural property - Surface protection for porous inorganic materials – Laboratory test methods for the evaluation of the performance of water repellent products. **2011**.
43. UNI EN 15802:2010. Conservation of cultural property - Test methods - Determination of static contact angle. **2010**.
44. UNI EN 623-4:2005. Advanced technical ceramics - Monolithic ceramics - General and textural properties - Part 4: Determination of surface roughness. **2005**.
45. ISO 2813:1994. Paints and varnishes - Determination of specular gloss of non-metallic paint films at 20 degrees, 60 degrees and 85 degrees. **1994**.
46. UNI EN 15886:2010. Conservation of cultural property. Test methods. Colour measurement of surfaces. **2010**.